Aircraft Tolerance Optimization Considering Quality, Manufacturing & Performance

Kanwardeep Singh Bhachu[1], Garrett Waycaster[2], Raphael T. Haftka[3], Nam-Ho Kim[4]

University of Florida, PO Box 116250 Gainesville, FL 23611-6250

Abstract

Manufacturing tolerance allocation is a design challenge that plays an important role in balancing the cost and weight objectives for an aircraft. The purpose of this paper is to explore an approach to optimize manufacturing tolerances by combining the individual objectives of the quality, manufacturing and design teams. We illustrate this approach on a fatigue critical lap joint structure that consists of a wing spar and a strap that must tolerate the manufacturing errors associated with location and size of the fastener holes. These errors are modeled with industrial data collected from the wing assemblies of a business jet. A cost model is formulated in terms of the quality cost, manufacturing cost and performance cost, and optimal tolerance is found by minimizing the sum of these costs (i.e. total cost). It was found that as the aircraft size grows bigger the weight increases more quickly than the quality cost requiring the use of tighter tolerance. A sensitivity analysis is also performed to identify the input variables that have significant impact on the optimal tolerance and corresponding total cost.

Nomenclature

d	=	Fastener hole diameter
e	=	Fastener edge distance
h	=	Spar height
L	=	Spar length
n_f	=	Total no. of fasteners
$n_{f\text{-}pf}$	=	Total no. of fasteners per foot
P_{QN}	=	Probability of quality notification
P_{CV}	=	Probability of constraint violation
t	=	Thickness
T	=	Tolerance
w	=	Width
w^0	=	Zero tolerance width
W	=	Weight
I_{ini}	=	Initial inspection interval
I^*_{ini}	=	Initial inspection constraint
C	=	Cost
ET	=	Engineering time
LT	=	Labor time
EC	=	Engineering cost (hourly)
LC	=	Labor time cost (hourly)
λ	=	Tradeoff ratio

[1] Graduate Research Assistant, Mechanical & Aerospace Engineering, and AIAA student member.
[2] Graduate Research Assistant, Mechanical & Aerospace Engineering.
[3] Distinguished Professor, Mechanical & Aerospace Engineering, and AIAA Fellow.
[4] Associate Professor, Mechanical & Aerospace Engineering, and AIAA Associate Fellow.

I. Introduction

The growing customer demand for low cost and efficient aircrafts requires manufacturers to deal with various design challenges early in the design phase. Manufacturing tolerance allocation is a design challenge that plays an important role in balancing the conflicting objectives of the quality, manufacturing and design teams. For given manufacturing technology the only input from manufacturing is the material cost. In such situations, a qualitative representation of the trade-off existing between these players is shown in Figure 1.

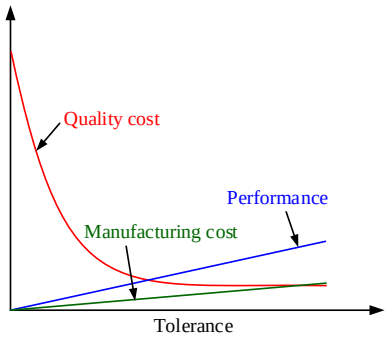

Fig. 1 Trade-off between various players

The manufacturing cost increases with the increase in tolerance as more material is needed to manufacture the same part. The quality cost decreases with the increase in tolerance. It can be defined as the cost incurred due to nonconformance of the manufactured part with the design specifications. For example in Figure 2, a fastener hole is designed to be at the center of the plate (i.e. edge distance of $w^0/2$) but due to manufacturing errors it can deviate and may violate a design constraint (e.g. fatigue life, allowable stress etc.) and require repair, which is the part of the quality cost. In order to reduce the need for repair, tolerance (T) is added to both edges of the plate as shown in Figure 2 (a). It helps in reducing the number of nonconforming events and thus reduces the quality cost. Another interpretation of tolerance is shown in Figure 2(b), where no quality problem will be encountered as long as the center of the hole remains within upper limit (UL) and lower limit (LL), provided that fastener diameter remains same.

However, width of the plate increases due to tolerance addition (i.e. width increases from w^0 to w) that leads to increase in the structural weight and hence degrade the performance of the aircraft. We model performance loss in terms of the extra money that customers have to pay due to increased structural weight attributable to the addition of tolerance.Therefore, increasing the tolerance increases the manufacturing cost and performance cost, whilst reducing the quality cost. In this paper we study the optimal compromise tolerance for a simple lap joint structure.

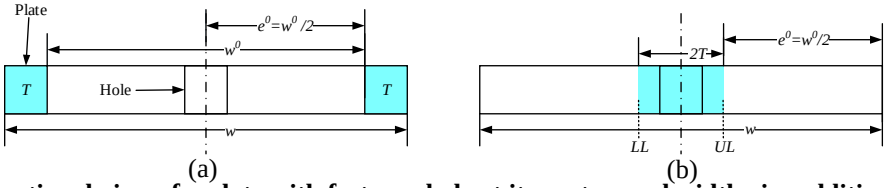

Fig. 2 Cross-sectional view of a plate with fastener hole at its center, and widthwise addition of tolerance.

Most tolerance allocation techniques only focus on minimizing the manufacturing cost without considering the quality cost [1,2]. A few methods allocate tolerance by balancing both manufacturing and quality costs [3,4]. Even fewer techniques account for the concurrent effect of tolerance on the performance, quality and manufacturing cost. Curran *et al*. [5] investigated the influence of tolerance on the direction operating cost (DOC) of an aircraft by extrapolating the results from the study performed on engine nacelle structure, and showed that relatively small relaxation in the tolerances resulted in reduced costs of production that lowered the DOC. Furthermore, Kundu and Curran[6] proposed a concept of global 'Design for Customer' approach that conjoins various individual design for customer approaches, such as 'Design for Performance', 'Design for Quality', 'Design for Cost', 'Design for Safety" to allocate the manufacturing tolerances.

We explore a similar 'Design for Customer' approach that combines inputs from manufacturing, quality, and performance for optimizing the manufacturing tolerances. That is, performance cost (C_P), quality cost (C_Q), and manufacturing cost (C_M) are summed to make an objective function of total cost (C_{total}). The primary objective is to

find a tolerance value that minimizes the total cost. A sensitivity analysis is also performed the input variables that can significantly impact the optimal tolerance and corresponding total cost. We illustrate this integrated approach on a single shear lap-joint structure discussed in the following section.

II. Design of a Lap Joint for Damage Tolerance

We consider the design of a lap joint for damage tolerance (i.e. fatigue resistance) as a demonstration for the manufacturing tolerance optimization procedure. Lap joints are widely on aircraft structures for attaching various parts together by using fasteners. A real example of such a lap joint is shown in Figure 3(a) that connects the two wing spars (from left and right wing) together with the help of strap and fasteners. Such joints are typically in double or triple shear but for simplicity we have assumed it to be in single shear. The simplified cross-sectional geometry representative of the real spar is shown in Figure 3(b).

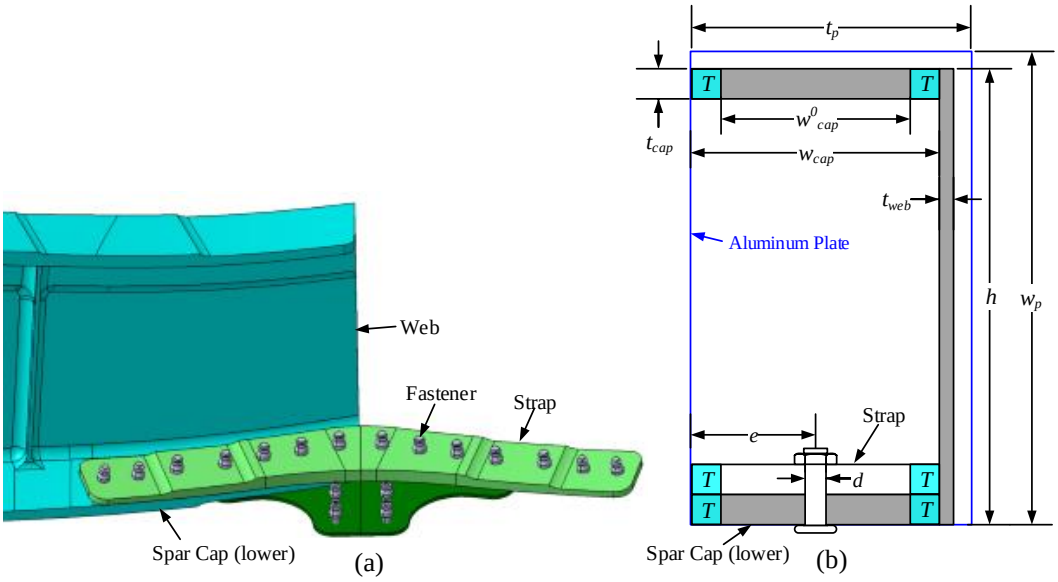

Fig. 3 (a) Wing spars (right spar not shown) connected by a lap joint, (b) Simplified cross-sectional geometry

The spar is assumed to be machined from 7475 -T761 aluminum alloy plate that is typically used to design fatigue critical parts because of its superior crack growth characteristics. The spar is further assumed to be 25 feet long, which is about half the wing span of a typical light business jet, and the other dimensions (i.e. cap thickness, cap width, web thickness and web height) are assumed to remain constant along the spar length. The dimensions assumed for the simplified geometry are listed in Table 1 and they approximately yield the same weight (i.e. 60 lbs.) as that of an actual spar shown in Figure 3(a). The strap connecting the two spar caps is also assumed to be made from 7475 - T761 aluminum alloy but it is not used in the cost calculations because its weight is negligible in comparison to the spar.

Table 1 Dimensions of the aluminum plate and machined spar

Aluminum Plate		Machined Spar	
Dimension	Value (in.)	Dimension	Value (in.)
Plate width, w_p	10.1	Zero tolerance cap width, w^0_{cap}	3.500
Plate thickness, t_p	4.00	Cap thickness, t_{cap}	0.165
Spar length, L	300	Spar height, h	10.00
-	-	Web thickness, t_{web}	0.080

Damage tolerant design and manufacturing errors

The objective of the damage tolerant design methodology is to ensure that cracks (e.g. present at the fastener holes) do not grow to a size that could impair the flight safety during the expected lifetime of an aircraft. It is done by specifying structural inspection intervals so that cracks could be found and replaced. A manufacturer has to show

that specified inspection intervals would satisfy this requirement by performing a crack growth analysis at every fastener hole.

Due to manufacturing errors, fastener holes can get mislocated and/or oversized as shown in Figure 4, and that may lead to nonconformance with the desired inspection interval constraints. Generally, multiple inspection intervals are defined throughout the service life of an aircraft, but we only consider the initial structural inspection interval I^*_{ini} that is assumed to be set at 12,000 flight hours (FH). In actuality, the manufacturer identifies such deviations and checks if they do violate any inspection interval constraint, and take action (such as repair or scrapping) if they do. So, we simulate (for our example spar lap joint) this procedure in the presence of simulated manufacturing errors (shown in Figure 4) by executing crack growth analyses at a fastener hole.

A common way to describe, record, and monitor the manufacturing errors/deviations/quality problems is 'Quality Notification (QN)'. This is a term specifically used by SAP software to refer to quality problems. A major task accomplished under QN review is the analysis and resolution of a quality problem by the concerned engineers. If the outcome of the engineering analysis (crack growth analysis in our case) shows that inspection constraint is not violated then a repair is carried out, otherwise a part (spar in this case) may have to be scrapped. A few examples of repairs are,

1. Plug and relocate the fastener hole while maintaining the specified edge distance.
2. Clean the hole to next available fastener diameter size and install the fastener.

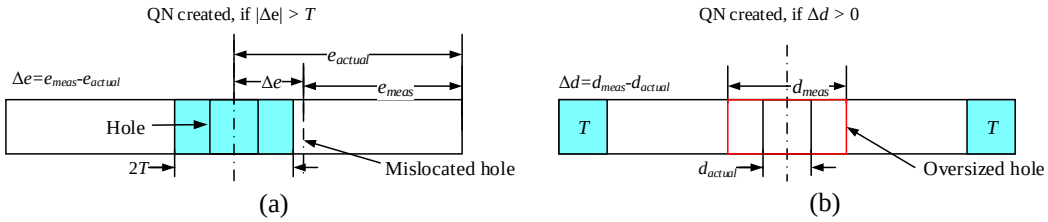

Fig. 4 (a) Edge distance deviation, (b) Hole diameter deviation

The scrapping of a high valued part such as spar ($ 10,000 – 15,000) is the least desirable. Consequently, it may be desirable to allocate an extraneous tolerance to the spar caps and strap as shown in Figure 3 (b). It would reduce the chance of constraint violation and hence the quality cost, but at the same time it leads to undesirable increase in weight. The weight increase increases the performance cost that is largely borne by the customers. The manufacturing cost will also increase because of the need for wider aluminum plates. Therefore, it is important to select a tolerance value that balances all the three cost components, i.e. quality cost, manufacturing cost and performance cost.

Crack growth analysis

We have performed crack growth analyses by using a free version of AFGROW (Air Force Growth, Version 4.0012.15). It is a fracture mechanics and fatigue crack growth analysis software tool that is widely used in the aerospace industry for design and analysis of the fatigue critical structures. In order to execute a crack growth analysis we have further simplified the spar structure shown in Figure 3 (b) into the structure shown in Figure 5.

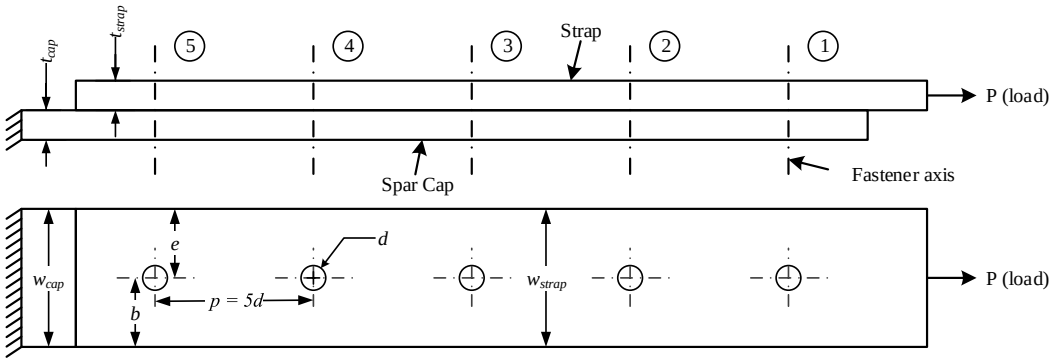

Fig. 5 Simplification of spar lap joint to execute crack growth analysis

We have assumed that strap and spar cap have same width and thickness (i.e. $w_{strap} = w_{cap} = w$ and $t_{strap} = t_{cap} = t$). All the fasteners are assumed to have same diameter d while maintaining the same edge distance $e = w/2$ and fastener pitch $p = 5d$. The axial load P (due to wing up-bending) is transmitted from the lower spar cap to the strap via fastener shearing. We have used an actual wing stress spectrum that came from a particular location on the lower spar cap of a business jet wing to execute the analyses. Note that crack growth analyses are only performed for the end fastener to calculate P_{CV} and then it is assumed that all the fasteners on the wing spar have same value of P_{CV}. More information about crack growth analysis can be found in Appendix (b).

III. Data and Distributions

The proposed integrated tolerance optimization scheme treats the two types of manufacturing deviations/errors (shown in Figure 4) as random variables. The edge distance deviation Δe is a continuous random variable, while hole diameter deviation Δd is a discrete random variable. The physical data for the two random variables were collected from the wing assemblies of a business jet with the help of Cessna Aircraft Company. These data are used to estimate the distributions for each random variable in order to estimate the probability of encountering a quality notification P_{QN} and probability of violating an inspection constraint P_{CV}. These probability estimates are used in the cost model to calculate the expected value of the quality cost C_Q.

Edge distance distribution (EDD)

The edge distance deviation data Δe were collected from the lower spar caps of the 8 wing assemblies of a business jet. A total of 8164 samples were fitted with 12 continuous parametric distributions available in MATLAB (Normal, Lognormal, Logistic, Log Logistic, Weibull, Beta, Generalized Extreme Value, Gamma, Inverse Gaussian, Nakagami, Rician, and Birnbaum-Saunders). The goodness of fit was checked with the two-sample Kolmogorov-Smirnov (K-S) test that rejected the hypothesis (at 5% level of significance) that fitted distribution and data belong to the same distribution. However, visual inspection of the quantile-quantile (Q-Q) plot shown in Figure 5 (a) indicate that logistic distribution may be a good candidate as it departs little from the data in comparison to the other distributions (only normal distribution is shown for comparison). The maximum likelihood estimates (MLE) of the distribution parameters are listed in Table 2. The cumulative density function of the logistic and normal distribution are given as follows,

$$F(x) = \frac{1}{1 + e^{-\frac{x-\mu}{s}}} \text{(Logistic)}, \tag{1}$$

$$F(x) = \frac{1}{2}\left[1 + \text{erf}\left(\frac{x-\mu}{\sqrt{2}s}\right)\right] \text{(Normal)}. \tag{2}$$

Table 2 Maximum likelihood parameter estimates of logistic and normal distribution

	Logistic	Normal
Parameters	(inch)	(inch)
Location (μ)	-0.00055	-0.00079
Scale (s)	0.01378	0.02477

Since quality notes are generated by the tails of the distribution, the deviation of the data from the distribution in the tail region may lead to substantial errors. In order to get more accurate representative distribution in the tail region, we fitted the measured data with a semiparametric distribution. The central region of the distribution is estimated by the piecewise linear non-parametric estimate of the CDF and both tails are fitted with the generalized Pareto distribution. The Pareto tails were fitted at the cumulative probabilities of 0.01 (-0.0622") and 0.99 (0.066"). The cumulative probabilities used to fit distribution were selected based on visual inspection. However, finding the combination of cumulative probabilities that minimizes the departure from linearity at the tails is an optimization problem in itself, which will be investigated later as a part of our future work.

The Q-Q plot of the actual data and data generated from semiparametric fit is shown in Figure 5 (b). It indicates a very little deviation from the data signifying that semiparametric distribution fits the data better than the logistic and normal distributions. We also performed the two-sample K-S test (at 5% significance level) and it supported the hypothesis that semiparametric distribution and actual data belongs to the same distribution. So, we have used the semiparametric fit to estimate the P_{QN} and P_{CV} used in the calculation of quality cost during tolerance optimization.

However, logistic distribution is used in the sensitivity analysis to illustrate the impact of uncertainty in edge distance deviation data on the optimal tolerance by simply varying the scale parameter *s* of the distribution.

Because the semiparmetric distribution fit the tail well, there is hope that it extrapolates well for extreme deviations that were not observed in the actual data. For example, the lower half portion of the CDF (i.e. cumulative probabilities between 0 and 0.5) for each of the three distributions is shown on log scale in Figure 6. The logistic distribution over predicts the probabilities at the tail (i.e. 10^{-5} – 10^{-8}) particularly beyond the maximum observed deviation of -0.128", which essentially means that there is a finite probability of observing deviations (< -0.15 or > 0.15) that are practically impossible. On the other hand, normal distribution under predicts the probabilities at the tail i.e. between line A and B the probabilities quickly fall from 10^{-2} to 10^{-7} that too is inaccurate.

However, semiparametric distribution gives higher probabilities of the all between line A and B, which means that it gives more emphasis to the tails. It also allows to predict the deviations in excess of -0.128" up to about -0.15" with finite probabilities ranging from 10^{-5} to 10^{-8} that are practically possible. It will be shown later that it is worth investing effort in tail modelling as use of logistic fit in estimating P_{QN} leads to non-optimal tolerance.

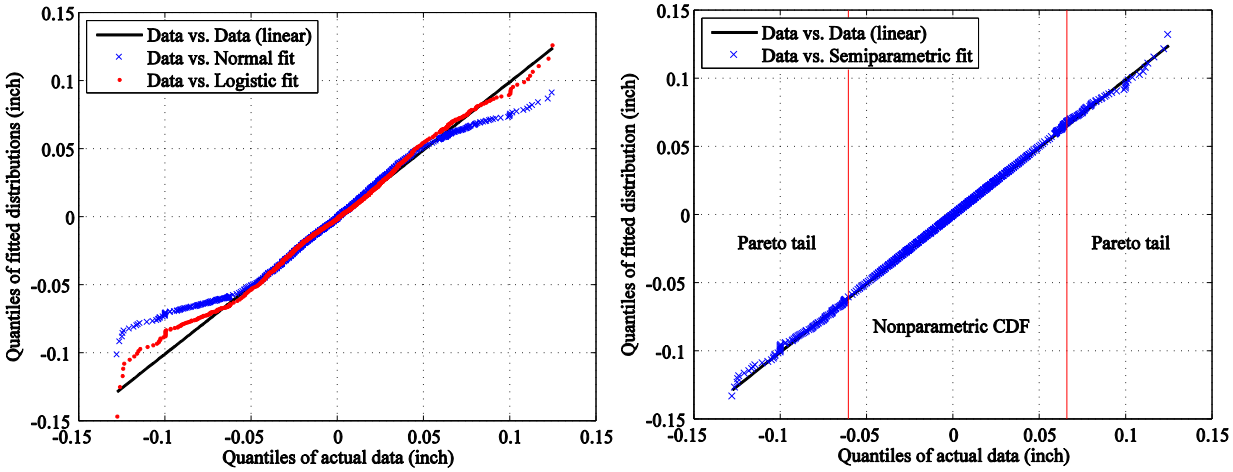

Fig. 6 (a) Q-Q plot of actual data vs logistic and normal fits, (b) Q-Q plot of actual data vs semiparametric fit.

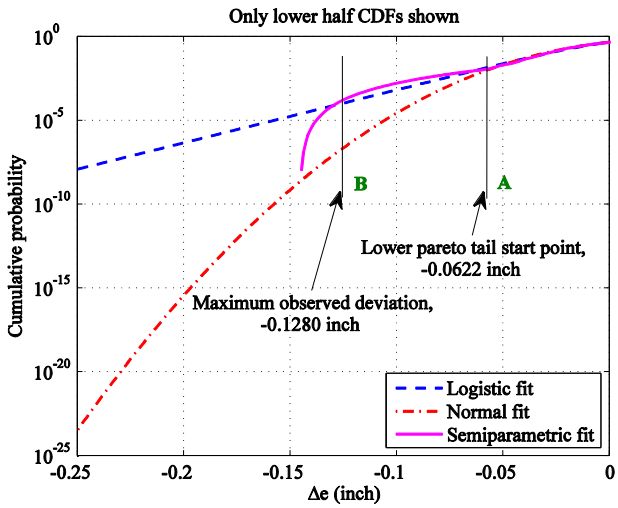

Fig. 7 CDF of logistic, normal and parametric fit

Hole diameter deviation distribution (HDD)

The hole diameter deviation data Δd were collected from the wing assemblies of about 110 airplanes with sample size of 650,642. Aerospace fasteners are generally available in Δd =1/64" increments, i.e. if d = 8/32" fastener gets oversized due to manufacturing error then the next available fastener size is 8/32"+1/64" and so on. This makes the hole diameter deviation a discrete random variable. So, we have used a simple histogram to

represent the distribution. The probabilities associated with 13 subsequent fastener increments are listed in Table 3 and the probability that a fastener will be oversized is $P(\Delta d > 0) = 0.001724$ (i.e. 1122 out of 650,642).

Table 3. Fastener oversize (hole diameter deviation) probabilites

Oversize, Δd (inch)	Probability	Oversize, Δd (inch)	Probability	Oversize, Δd (inch)	Probability
0/64	9.98E-01	5/64	6.61E-05	10/64	3.07E-06
1/64	1.54E-04	6/64	9.84E-05	11/64	1.54E-06
2/64	1.02E-03	7/64	2.61E-05	12/64	3.07E-06
3/64	1.38E-04	8/64	1.08E-05	13/64	1.54E-06
4/64	1.83E-04	9/64	1.54E-05	-	-

IV. Estimating Probabilities

The probability of quality notification and probability of constraint violation are estimated by using the distributions estimated above to calculate the expected value of quality cost. The procedure for estimating these probabilities is discussed next.

A. Probability of Quality Notification (P_{QN})

A QN is created when two types of fastener deviations exceed certain values i.e. when edge distance deviation exceeds the allocated tolerance value (i.e. $|\Delta e| > T$) and/or hole diameter deviation is greater than zero (i.e. $|\Delta d| > 0$). It is assumed that both the events are uncorrelated and independent of each other. Therefore, it allows the calculation of P_{QN} (per fastener) by using the following formula,

$$P_{QN} = P(|\Delta e| > T) + P(\Delta d > 0) - P(|\Delta e| > T)P(\Delta d > 0)\,. \tag{3}$$

Where, $P(|\Delta e| > T)$ is first estimated by using a logistic fit (case 1) and then by semiparametric fit (case 2), and $P(|\Delta d| > 0)$ is fixed at 0.001724 in both the cases as it does not change with tolerance. The P_{QN} estimated for each case is shown as a function of tolerance in Figure 7 (a), and difference (ΔP_{QN}) between them is shown in Figure 7 (b).

In both cases, the P_{QN} starts off at 1 when no tolerance is added and reduces to about 1.72E-3 (the contribution of errors in hole diameters) after a tolerance of 0.13". P_{QN} for case 1(logistic fit) deviates significantly from case 2(semiparametric fit) between 0 – 0.12" tolerance but the difference falls below 1E-4 after 0.13" tolerance. It is due to the fact that $P_{QN} \approx P(|\Delta d| > 0)$ after 0.13" tolerance that is same in both the cases. The values of P_{QN} estimated for case 2 (semiparametric fit) are listed in Table 4.

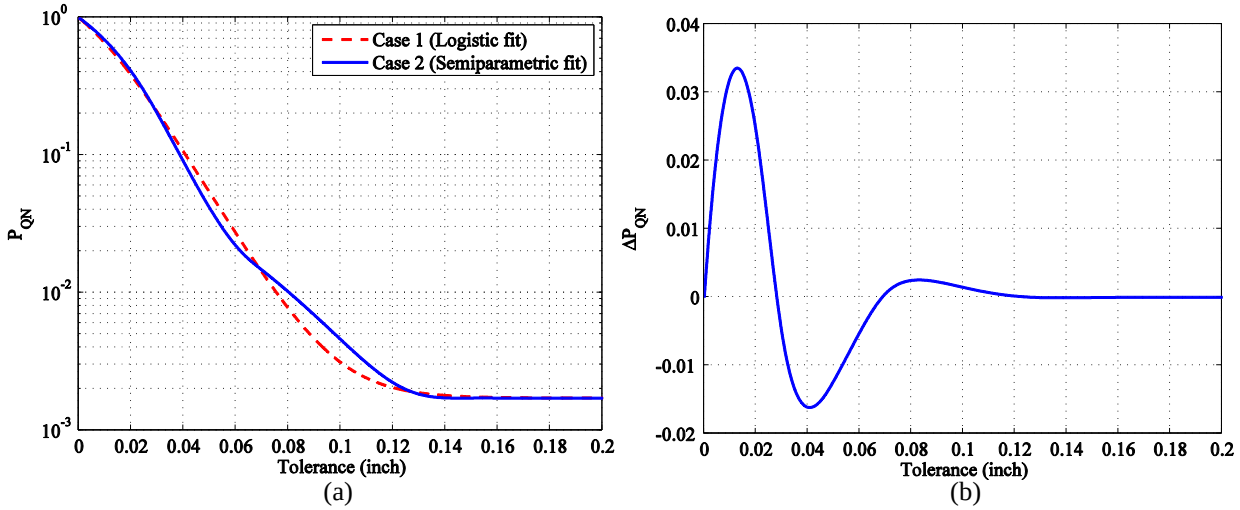

(a) (b)

Fig. 8 (a) P_{QN} variation with tolerance for case 1 and case 2, (b) The difference between the two cases, ΔP_{QN}

Table 4 P_{QN} estimates at each tolerance value for case 2 (semiparametric fit)

T(in.)	P_{QN}	T (in.)	P_{QN}	T (in.)	P_{QN}
0.00	1.00E+00	0.07	1.46E-02	0.14	1.72E-03
0.01	6.85E-01	0.08	1.02E-02	0.15	1.72E-03
0.02	4.05E-01	0.09	6.90E-03	0.16	1.72E-03
0.03	2.00E-01	0.10	4.59E-03	0.17	1.72E-03
0.04	8.96E-02	0.11	3.09E-03	0.18	1.72E-03
0.05	4.12E-02	0.12	2.23E-03	0.19	1.72E-03
0.06	2.20E-02	0.13	1.84E-03	0.20	1.72E-03

B. Probability of Constraint Violation (P_{CV})

The constraint is violated when an initial inspection interval I_{ini} estimated from crack growth analysis fails to meet the initial inspection constraint of I^*_{ini}=12,000 flight hours (FH). In the event of constraint violation, a few repair options available (e.g. cold working a hole) are available that can bring the calculated crack growth life above 12,000 FH depending upon the severity of constraint violation. However, in order to simplify the analysis and modeling we have assumed that a spar will be scrapped if the initial inspection constraint is violated. The estimated initial inspection interval is calculated by dividing the total crack growth life (N_f) by a factor of two i.e. $I_{ini} = N_f/2$.

The probability of constraint violation is calculated by performing Monte Carlo Simulation (MCS). The MCS in essence simulates a QN reviewing process, where a given combination of fastener deviation $\{\Delta e, \Delta d\}$are checked for the possibility of constraint violation by executing a crack growth analysis.

Monte Carlo Simulation

The estimate of P_{CV} for a single fastener by Monte Carlo Simulation requires millions of crack growth analyses to be performed with each analysis corresponding to a set of fastener deviations randomly generated from their respective distributions. A particular sample set fails to meet the inspection constraint if,

$$I_{ini} - I^*_{ini} < 0, \text{ or } \frac{N_f}{2} - 12000 < 0, \text{ where } N_f = f(\Delta d, \Delta e) . \tag{4}$$

Then, P_{CV} is simply estimated by dividing the number of sample sets that fail to meet the initial inspection constraint by the total number of sample sets,

$$P_{CV} = P(I_{ini} < I^*_{ini}) \approx \frac{n_{fail}}{n_{total}} . \tag{5}$$

The standard error in MCS is estimated by the following equation,

$$SE = \sqrt{\frac{P_{CV}(1-P_{CV})}{n_{total}}} . \tag{6}$$

An example of the interpolation functions is shown in Figure 9 that shows Δd on the x-axis and Δe on y-axis and I_{ini} *on* z-axis. In figure 9 (A) that corresponds to the zero tolerance (i.e. $T = 0.0$"), notice that only point A has initial inspection slightly greater than 12,000 FH (constraint shown by a plane), that indicates that slight deviation in Δe and Δd leads to the constraint violation, e.g. point B that has $\Delta e = 0.025$" and $\Delta d = 0$" violates a constraint as it falls below the constraint plane. Subsequently, tolerance is added in 0.01" steps, so that new width w becomes $w^0 + 2T$. The effect of tolerance addition can be noticed from Figure 9 (b) where entire surface shifts upward bringing more points above the constraint plane. Thus, reduction in P_{CV} with increase in tolerance is evident.

Although, AFGROW takes only about 2-3 seconds to execute a single crack growth analysis but it is impractical to execute 10 million analyses. So, we have used 2-D interpolation functions shown in Figure 9 to estimate the initial inspection interval for the randomly generated deviation sample sets. Total of 21 interpolation function were used with each corresponding to the subsequent addition of tolerance T in 0.01" steps starting from 0"

to 0.2". The deviation sample space (Δe, Δd) contains total of 126interpolation points/nodes (9 points along Δe and 14 points along Δd) that are used to execute the actual crack growth analyses.

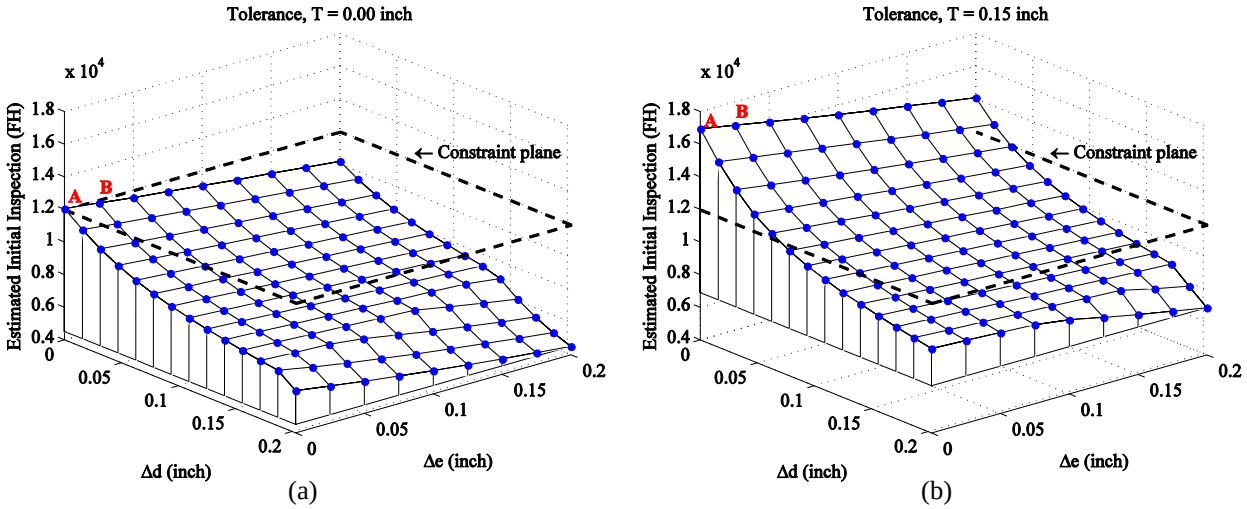

Fig. 9 (a) Interpolation function for zero tolerance width, (b) Interpolation function for tolerance T = 0.15"

The root mean square error (RMSE) of the interpolation ranged between 16-19 flight hours (FH) all the 21 interpolation functions. In order to check the impact of this error on the P_{CV} calculation, 50000 AFGROW analyses were performed that resulted in the same value of P_{CV} as that by the interpolation function. Refer to Appendix A for more details about the interpolation accuracy. The plot of P_{CV} as a function of tolerance is shown in Figure 10 (a) for both the cases, and difference ΔP_{CV} between the both is shown in Figure 10 (b). It can be noticed from Figure 10 (b) that ΔP_{CV} becomes less than 1.0E-4 after 0.05" tolerance indicating that for larger tolerances constraint violation is being dominated by the hole diameter deviation that is same in both the cases. The values of P_{CV} estimated for case 2 (semiparametric fit) are listed in Table 5.

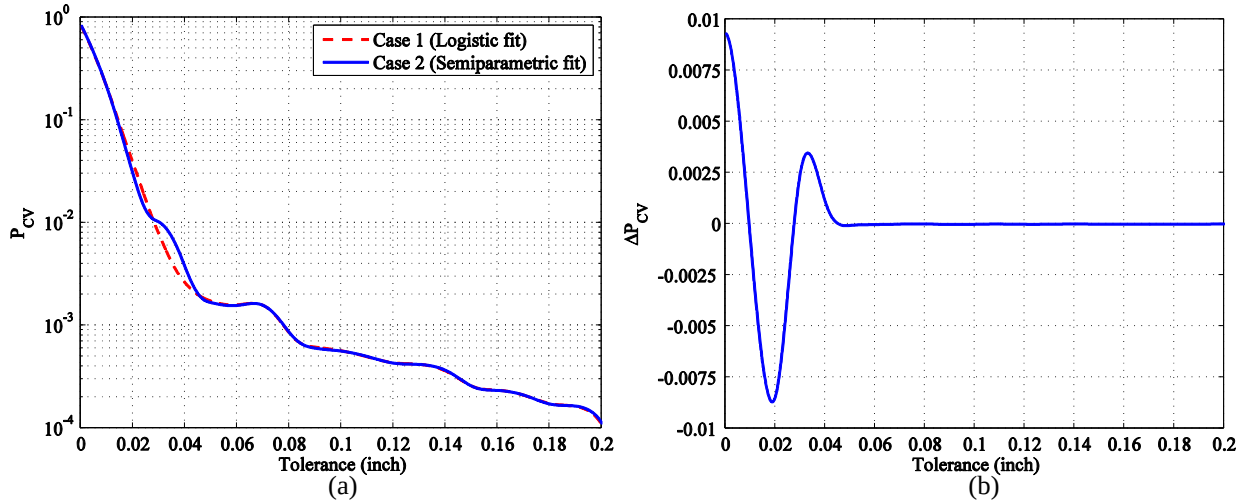

Fig.10 (a) P_{CV} variation with tolerance for case 1 and case 2, (b) The difference between the two cases, ΔP_{CV}

Table 5 P_{CV} estimates at each tolerance value for case 2 (semiparametric fit)

T (in.)	P_{CV}	SE	T (in.)	P_{CV}	SE	T (in.)	P_{CV}	SE
0.00	8.44E-01	1.15E-04	0.07	1.58E-03	1.25E-05	0.14	3.69E-04	6.07E-06
0.01	2.06E-01	1.28E-04	0.08	8.58E-04	9.26E-06	0.15	2.59E-04	5.09E-06
0.02	2.97E-02	5.37E-05	0.09	6.05E-04	7.77E-06	0.16	2.35E-04	4.84E-06
0.03	1.02E-02	3.18E-05	0.10	5.67E-04	7.53E-06	0.17	2.12E-04	4.60E-06
0.04	3.69E-03	1.92E-05	0.11	5.02E-04	7.08E-06	0.18	1.73E-04	4.16E-06
0.05	1.68E-03	1.29E-05	0.12	4.33E-04	6.58E-06	0.19	1.65E-04	4.06E-06
0.06	1.58E-03	1.26E-05	0.13	4.20E-04	6.48E-06	0.20	1.13E-04	3.36E-06

V. Cost Model

We have developed a cost model that consists of the three major components, i.e. quality cost, manufacturing cost and performance cost. The total cost is expressed as the sum of these three cost components that is minimized to find the optimal tolerance. Various individual components of the cost model are discussed as follows.

A. Quality Cost (C_Q)

Quality cost captures the expense incurred due to review of a quality notification (QN). The outcome of a review may either lead to a repair (corrective action) or constraint violation (part scrapping) that constitutes the quality cost as shown in the flowchart below.

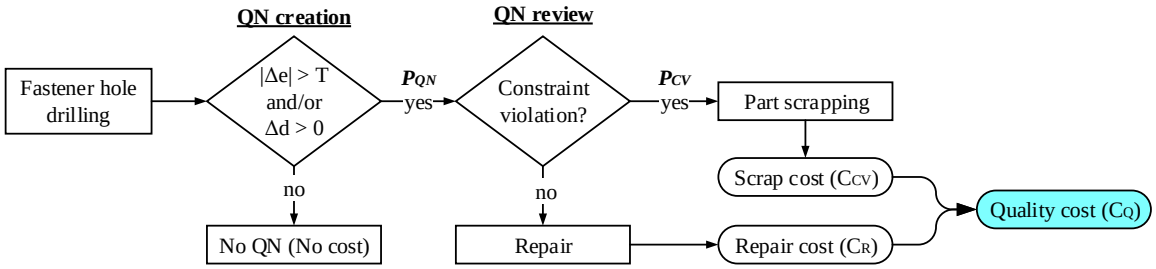

Fig. 11 Flowchart showing various components of quality cost

Therefore, the two major components of the quality cost are repair cost C_R and constraint violation/scrap cost C_{CV}. It gives rise to the following equation,

$$C_Q = C_R + C_{CV}. \tag{7}$$

The repair cost captures the cost associated with resolving all the QNs that does not lead to constraint violation. The cost of materials and tools used in most of the repairs is negligible. So, we have modeled the repair cost in terms of the human resources used during the complete process i.e. engineers are required to review and specify a repair and labor is used to execute a repair. The following equation is used to estimate the repair cost,

$$C_R = n_f P_{QN} C_{QN} = n_f P_{QN} \left[(EC)(ET) + (LC)(\mathrm{LT})\right]. \tag{8}$$

Where, C_{QN} is the average cost of quality notification for a single fastener; EC ($ 100) and LC ($ 65) are the average hourly engineering and labor cost; ET (3/4 hr.) and LT (1/2 hr.) are the average engineering and labor time involved in resolving a single QN; P_{QN} is the probability of QN creation and n_f is the total number of fastener holes to be drilled in a spar. The cost of constrain violation is mainly the scrap cost that is estimated by the following expression,

$$C_{CV} = 2P_{CV} W_p C_{Al} = 2P_{CV} \left(w_p t_p L \rho_{Al}\right) C_{Al}. \tag{9}$$

Where, C_{Al} is the cost for a pound of aluminum alloy (5.50 $/lb.); W_p is the weight of raw aluminum plate; P_{CV} is the probability of violating an inspection interval constraint. A factor of 2 is used in the equation because raw

material cost for the high valued parts (such as wing spar) is generally about 50% of the total scrap cost. The final equation for the quality cost is found by plugging Eq. (9) and Eq. (8) into Eq. (7),

$$C_Q = n_f P_{QN}\left[(EC)(ET)+(LC)(\mathrm{LT})\right]+2P_{CV}\left(w_p t_p L\rho_{Al}\right)C_{Al}\,. \tag{10}$$

B. Manufacturing Cost (C_M)

The two main constituents of C_M are tooling cost and material cost. As tooling cost is assumed to be constant (i.e. jigs, tools and technology remains the same), which means that tooling cost does not vary with the tolerance and therefore it can be taken out from the following equation,

$$C_M = \cancel{C_{Tool}} + C_{Mat} = C_{Mat}\,. \tag{11}$$

On the other hand, material cost is proportional to the weight increase ΔW_p of the raw aluminum plate multiplied by the cost per pound of the aluminum alloy C_{Al}. The increase in weight is calculated with respect to the zero tolerance design. It leads to the following expression for C_M,

$$C_M = C_{Mat} = \Delta W_p C_{Al} = \left(2hLT\rho_{Al}\right)C_{Al}\,. \tag{12}$$

C. Performance Cost (C_P)

It is the extra money that customers have to pay due to increased structural weight attributable to the addition of tolerance. It is aimed at measuring the direct impact of weight increase on the customer i.e. we call the addition of the performance cost into total cost as implicit customer modeling.

The maximum takeoff weight of an airplane can be divided into operational empty weight (OEW) and useful load as shown in Figure 11. We have slightly modified the breakdown of the OEW to put everything that does not take flight loads (inclusive of engines) under non-structural weight. The tolerance is added to the structural weight, and useful load is the sum of full fuel load and full fuel payload (i.e. passengers, crew, baggage etc.).We have assumed that maximum take-off weight (MTOW) of an airplane remains constant i.e. addition of tolerance increases the structural weight leading to reduction in the useful load capacity. Conversely, weight savings due to tolerance optimization decreases the structural weight leading to increase in the useful load capacity.

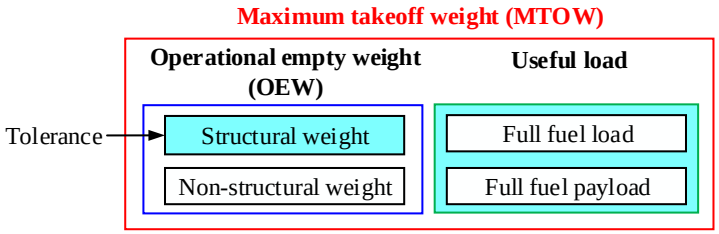

Fig.12 MTOW breakdown for an aircraft

The useful load of an aircraft is as an important characteristic that customers care about. The following equation expresses the performance cost as a function of increase in the spar weight ΔW_s due to addition of tolerance T and cost of useful payload C_{UL}. Again, weight increase is measured with respect to zero tolerance weight that leads to the following relationship for C_P,

$$C_P = \Delta W_s C_{UL} = \left(4t_{cap} LT\rho_{Al}\right)\left(\frac{S_{price}}{W_{useful}}\right). \tag{13}$$

Where, C_{UL} is the cost that customers pay for a pound of useful load. A reasonable measure of it can be calculated by dividing the sales price S_{price}[7] of an aircraft with useful load W_{useful} for the existing airplane models. A plot of C_{UL} calculated for various business jets is shown in Figure 13 with aircrafts arranged according to the increasing useful load capacity (weight data extracted from their respective websites). An example of the cost and weight data is given in Table 6. For our calculations we have used the average value of 1,200 $/lb.

Table 6 Weight and cost data for a business jet

Cessna Citation CJ 4	
MTOW, lbs	17110
Full fuel payload, lbs	1052
Full fuel load, lbs	5828
Useful load, lbs	6880
Sales price ($, million)	8.76
Cost of useful load ($/lb)	1273

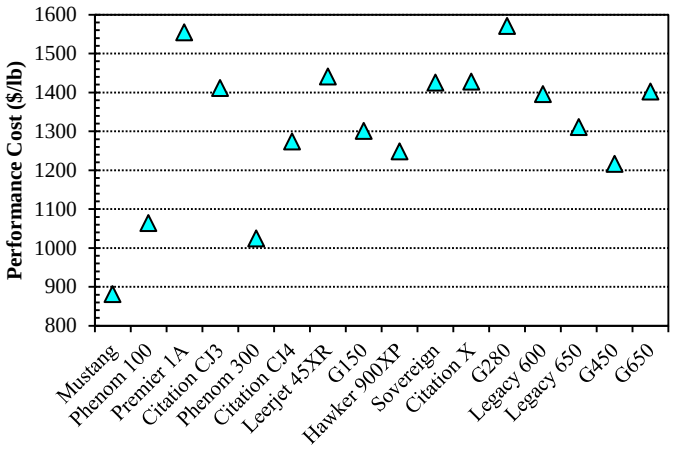

Fig. 13 Performance cost estimated for various business jets

D. Total Cost (C_{total})

It is used to represent the integrated cost function that combines all the individual cost objectives into a single cost objective that is used to optimize the tolerance is expressed by the following equation,

$$C_{total} = \underbrace{C_Q + C_M}_{C_{prod}\,(\text{Production cost})} + C_P . \tag{14}$$

For our example problem, the above equation can be expanded into the following,

$$C_{total} = \underbrace{\Bigg[\overbrace{\underbrace{n_f P_{QN}\left[(EC)(ET)+(LC)(\mathrm{LT})\right]}_{C_R} + \underbrace{2P_{CV}\left(w_p t_p L \rho_{Al}\right)C_{Al}}_{C_{CV}} + \underbrace{\left(2hLT\rho_{Al}\right)C_{Al}}_{C_M}}^{C_Q\,(Quality\ cost)}\Bigg]}_{C_{prod}\,(Production\ cost)} + \underbrace{\left(4t_{cap}LT\rho_{Al}\right)C_{UP}}_{C_P} . \tag{15}$$

VI. Optimization Results

The optimization problem is very simple, because there is only one design variable, the tolerance T. The optimization starts with the stepwise addition of tolerance (0.01" steps) to the width of the spar caps and straps, such that new width w becomes w^0+2T. All the cost components are recalculated at each step in order estimate the total cost C_{total}. An optimal tolerance is found by minimizing the total cost function,

$$\begin{aligned} &\min\ C_{total} \\ &\text{s.t.}\ \ 0 \le T \le T^{ub} \end{aligned} \tag{16}$$

Where, $T^{ub} = 0.2$" is the upper bound on the tolerance.

Individual cost components

The optimization is illustrated in Figure 14, where various cost curves are plotted as a function of tolerance. The repair cost C_R and constraint violation/scrap cost C_{CV} decrease with the increase in tolerance and follows the same trend as shown by P_{QN} and P_{CV}. Also, C_R on the average is about 30 times larger than C_{CV} i.e. expected cost due to scrapping of the spar is much lower than C_R. As, a result quality cost C_Q and C_R almost overlap on each other. Notice that C_R does not decrease further after 0.13" tolerance, which due to the fact that a major component of P_{QN} after 0.13" tolerance comes from the probability of hole diameter deviation i.e. $P(\Delta d > 0)$, which is fixed at 0.001724, because all the hole diameter deviations are assumed to be reviewed no matter how much tolerance is added. Although, C_R can be further reduced by modifying a criterion under which QN is created, which will be addressed in a future study. On the other hand, C_M and C_P increase with the increase in tolerance due to addition of extra weight to the spar ΔW_s and aluminum plate ΔW_p. The ΔW_s curve depicting addition of extra weight is also shown in Figure 14 with corresponding values labeled on the right vertical axis e.g. spar weight increases by 4lbs. (approx.) due to addition of 0.2" tolerance.

Total cost and optimal tolerance

The total cost curve shown in Figure 14 is initially dominated by the quality cost characterized by a non-linear decrease up to 0.0643"tolerance, which is indeed the optimal tolerance (shown by a star) and it corresponds to the total cost of $ 2476. The total cost again starts to increase after the optimum tolerance and is dominated by the sum of performance cost C_P and manufacturing C_M cost thereafter. Therefore, optimization achieves the goal of finding a tolerance value that balances the three cost components i.e. performance cost, manufacturing cost and quality cost.

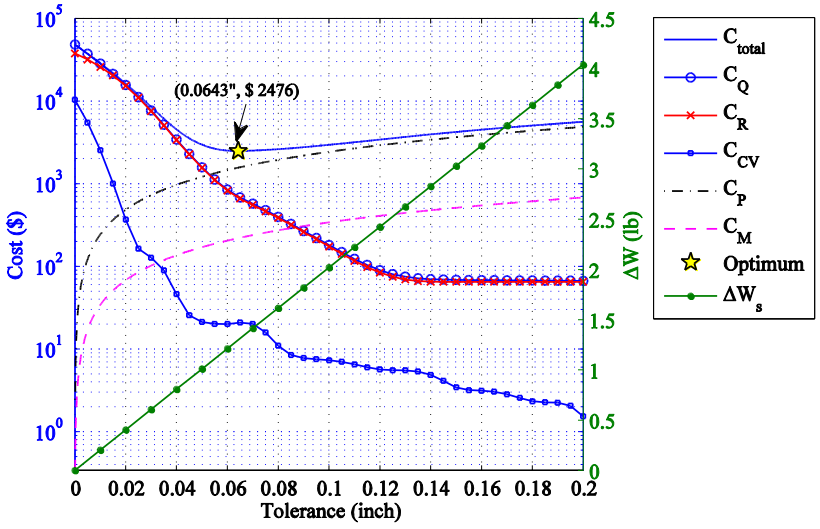

Fig. 14 Tolerance optimization showing total cost (C_{total}), quality cost (C_Q), repair cost (C_R), cost of constraint violation (C_{CV}), performance cost (C_P), manufacturing cost (C_M) and weight increase (ΔW_s) vs. tolerance.

A closer look at the region around the optimal tolerance as shown in Figure 15 reveals the scope for some flexibility to the manufacturer in relaxing or tightening the optimal tolerance without significantly increasing the total cost and structural weight. For example, optimum can be shifted to point A or B with only $ 28 or $30 increase in the total cost, accompanied by change -0.087 lb or 0.115 lb in weight. This kind of flexibility might be helpful to the manufacturer as it may allow them to retain tolerance commonality between similar parts without significantly increasing the total cost.

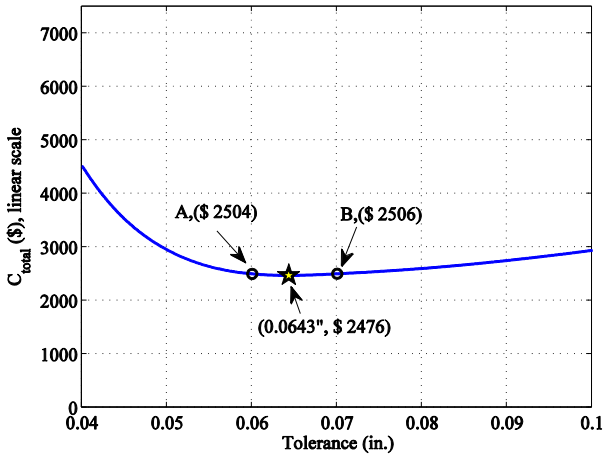

Fig. 15 Region around optimum showing flexibility in changing tolerance value.

Effect of distribution selection on optimal tolerance and total cost (logistic fit vs. semiparametric fit)

The semiparametric fit and logistic distributions were used separately in combination with hole diameter deviation data to estimate the P_{QN} and P_{CV}. The logistic fit (which is a less accurate fit to the edge distance deviation data) gives higher optimal tolerance value of 0.0732" than the optimal tolerance of 0.0643" given by the semiparmetric fit, i.e. 0.18 lb weight difference (Figure 16). However, both the optimums (optimum SPF and optimum LF) gave approximately same total cost i.e. the difference is of only $ 2. The reason for such a small difference in total cost is due to the fact that ΔP_{QN} is very small between 0.063" and 0.075" (refer to Figure 8 (b)).

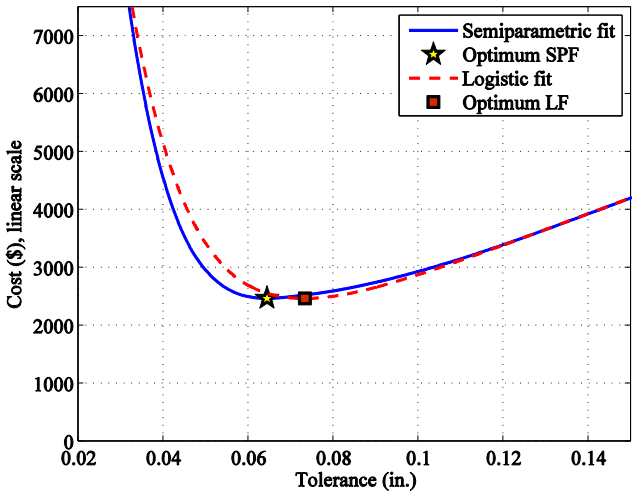

Fig. 16 Optimal tolerance values corresponding to the use of semiparametric and logistic fit

Importance of performance cost

In practice, the tolerances are specified mainly based on experience and most tolerance allocation approaches based on cost-tolerance modeling finds fairly limited usage in the industry[8]. It is possible that impact of tolerance allocation on weight might not get detailed attention. In order to illustrate the importance of detailed performance modeling we consider performing the optimization by only considering the combination of quality cost and

manufacturing cost, which is the case with the most cost-tolerance allocation approaches [1-4]. The Eq. (15) in such a case reduces to the following expression,

$$C_{prod} = \overbrace{\underbrace{n_f P_{QN}\left[(EC)(ET)+(LC)(\mathrm{LT})\right]}_{C_R} + \underbrace{2P_{CV}\left(w_p t_p L \rho_{Al}\right)C_{Al}}_{C_{CV}} + \underbrace{\left(2Th_p L \rho_{Al}\right)C_{Al}}_{C_M}}^{C_Q\,(Quality\ Cost)}. \quad (17)$$

Above relationship gives the production cost C_{prod} i.e. the cost to the manufacturer for producing a spar. In Figure 17, the C_{prod} can be seen to decrease with the increase in tolerance and reaches a minimum value of \$ 495 at 0.1145" tolerance value (i.e. optimum without performance cost). The C_{prod} then starts to increase with further addition of tolerance because increase in the manufacturing cost (due to materials) starts to dominate the quality cost.

In order to see more clearly the effect of including the performance cost, let us first mark a new point B in Figure 17 by vertically moving down the optimum (found by considering C_P) onto C_{prod} curve and mark point A by moving optimum (without considering the C_P) vertically upwards up to C_{total} curve.

Ignoring performance cost leads to a spar design that is approximately 1 lb heavier and costs \$423 lesser to the manufacturer on the C_{prod} curve i.e. difference between point B and optimum (excluding C_P) (\$ 918 -\$ 495).In which case, a customer will get an aircraft wing that is 6 lbs. heavier (assuming 6 spars in a wing) than the optimum found by considering C_P (shown by star) but \$ 2538 (6×\$ 423) cheaper. It is cheaper because manufacturer reduced its cost of production (sum of quality cost and manufacturing cost) that allows them to offer a wing at the reduced cost. Conversely, if performance cost is included in the cost model, a customer will get an aircraft wing that is 6 lbs. lighter than the optimum (excluding the C_P) but \$ 2538 (6×\$ 423) more expensive. It leads us to define a tradeoff ratio λ given by the following formula based on the optimal points shown in Figure 17,

$$\lambda = \frac{\left(\Delta W_{s-opt} - \Delta W_{s-opt(excludeC_P)}\right)C_{UL} - \left(C_{opt(excludeC_P)} - C_B\right)}{C_{opt(excludeC_P)} - C_B} = \frac{\left[\Delta(\Delta W_s)C_{UL}\right] - \Delta C_{prod}}{\Delta C_{prod}} = \frac{\text{Net Customer's loss}}{\text{Customer's gain}}. \quad (18)$$

Where, ΔC_{prod} is manufacturer's cost savings (that ultimately translates into customer's gain due to price reduction) when customer is not modeled i.e. the difference between optimum (excluding C_P) and point B;$\Delta(\Delta W_s)$ is the corresponding weight penalty that is translated into customer's loss when multiplied by the cost of useful load C_{UL} (1200\$/lb). The tradeoff ratio is basically the ratio of net customer's loss (difference between customer's loss due to weight increase and gain due to reduction in the production cost) to the customer's gain when performance cost is not modeled. A higher positive value of λ indicates that customer's net loss is much more that their gain. Note that λ is not intended to balance the customer's loss and manufacturer's gain, but to compare the effect of not considering the detailed treatment of performance cost in the cost model.

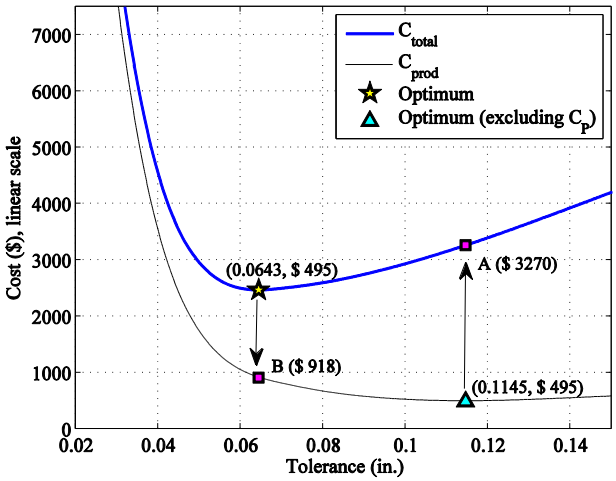

Fig. 17 Optimum tolerance when performance cost is modeled and not modeled

Effect of aircraft size on optimal tolerance and cost vs. weight tradeoff

We are interested in finding out what happens to the optimal tolerance, and trade off ratio λ with the change in aircraft category. We have considered three aircrafts A, B and C each belonging to the following categories based on their maximum takeoff weight (MTOW), very light jet, light jet, and mid-size business jet. The MTOW and estimated spar length for each of the three aircrafts is listed in Table 6, where aircraft B represents our base design. We have assumed that spar's cross-sectional area and volume follows the square/cube law i.e. weight of a spar increases by a cube of the change in the length and area of the cross-section increase by a square. For example, if length of the spar is increased by 2 times then rest of the dimensions also change proportionally leading to 8 times increase in the volume and weight. It is a reasonable assumption as indicated by F. A. Cleveland in his classic paper on size effects[9] showed that an increase in the weight of a wing approximately approaches the square/cube law. He also showed that weight of a wing varies approximately as the airplane gross weight (i.e. MTOW) to the power of 1.427, we have assumed it to roughly hold true for our wing spar giving rise to the following relationship,

$$\left(\frac{W^B_{MTOW}}{W^A_{MTOW}}\right)^{1.427} = \left(\frac{W^B_{wing}}{W^A_{wing}}\right) \approx \left(\frac{W^B_{spar}}{W^A_{spar}}\right). \tag{19}$$

The weight change predicted by using the square/cube law gives approximately similar results as by the above equation as shown in Table 7. The weight change is measured with respect to base design (B) for which spar weight is known to be about 60 lbs.

Table 7 Weight change prediction from square cube law and Eq. (19)

Aircraft	MTOW (lbs.)	Spar Length (ft.)	Spar Weight (lbs.) S/C law (Eq. 19)	Weight Change S/C law (Eq. 19)
A	10472	20.20	31.2 (30)	0.52 (0.50)
B	17110	25.05	60	-
C	30300	31.70	122 (136)	2.03 (2.26)

The following assumptions are used to generate the results,

1. Weight of the spar/wing follows a cubic change when scaled while holding the relative geometry constant.
2. Same material is used for all the spar sizes.
3. Similar manufacturing methods and assembly procedures are used, such that distributions for Δe and Δd remain the same.
4. Probability of constraint violation and all other cost inputs remains the same as that for the base design B.

The tolerance optimization is repeated for each spar size by recalculating all the relevant costs at each tolerance addition step of 0.01" followed by estimation of the cost values at much finer tolerance steps of 0.0001" by using 1D spline interpolation. The results of the optimization are shown in Table 8, which indicates that optimal tolerance decreases with the increase in spar size. It is because sum of C_P and C_M grows quicker than C_Q causing the optimal tolerance to decrease. Also, for the alternate formulation C_M grows quicker than C_Q leading to the decrease in optimal tolerance. So, for the bigger airplanes lower tolerance is needed whether or not a manufacturer models the performance cost. However, the tradeoff ratio λ calculated by using Eq.(18) increases with the increase of the spar size, which suggests that it becomes more important for the manufacturer to consider detailed modeling of the performance cost for bigger aircraft. For example, net customer's loss for aircraft C is 2.31 times more than what they gain from lowered production cost when performance cost was not modeled.

Table 8 Effect of spar size change on optimal tolerance and tradeoff ratio

	Optimum 1			Point B	Optimum 2					
Aircraft	Tolerance (in.)	C_{total} ($)	ΔW_s (lb.)	C_{prod} ($)	Tolerance (in.)	C_{prod} ($)	ΔW_s (lb.)	$\Delta(\Delta W_s)$ (lb.)	ΔC_{prod} ($)	λ
A	0.0669	1714	0.882	656	0.1175	337	1.549	0.667	319	1.51
B	0.0643	2475	1.298	917	0.1145	494	2.312	1.014	423	1.88
C	0.0618	3744	2.007	1336	0.1108	760	3.598	1.591	576	2.31

VII. Sensitivity Analysis

A sensitivity analysis is performed to evaluate the impact of uncertainties in the input variables on the optimal cost and corresponding total cost. The variables considered in the analysis are listed in Table 9 along with their nominal values, upper and lower bounds.

Table 9 Variables considered for the sensitivity analysis

Input variable	Unit	Lower bound	Nominal value	Upper bound
Cost of useful load, C_{UL}	\$/lb.	800 (-33.3%)	1200	1600 (33.3%)
Cost of quality note, C_{QN}	\$	53.75 (-50%)	107.5	161.25 (100%)
Cost of aluminum, C_{Al}	\$/lb.	2.50 (-55%)	5.5	11 (100%)
Scale of EDD distribution , s	in.	0.011(-20%)	0.0138	0.0207(50%)
Probability of hole over size, $P(\Delta d>0)$	-	0 (-100%)	0.001724	0.005173(200%)

The sensitivities are evaluated by calculating the logarithmic derivatives of the output $\psi(Y)$ and input $\psi(X)$, and then dividing the derivatives to get the sensitivity as follows,

$$\frac{\psi(Y)}{\psi(X)} = \frac{\Delta Y_i / Y_{nom}}{\Delta X_i / X_{nom}} = \frac{(Y_i - Y_{nom}) / Y_{nom}}{(X_i - X_{nom}) / X_{nom}}. \tag{20}$$

Sensitivity to uncertainty in the cost of useful load

The exact value of the cost of useful load is not known for a new aircraft early in the design phase. So, it is estimated by dividing the sales price of an aircraft by its useful load for the current similar aircrafts. The C_{UL} ranged between 800-1600 \$/lb for the current aircrafts as shown in Figure 13. We have used 1200 \$/lb (nominal value) to perform the optimization, but it is possible that the actual value of C_{UL} for the aircraft under consideration might be different. Therefore, it is important to evaluate the impact of uncertainty/error in the estimation of C_{UL} on the optimal tolerance and associated total cost.

The results of sensitivity analysis are presented in Table 10. We found that optimal tolerance is not quite sensitive to the uncertainty in C_{UL} i.e. for -33 % error in C_{UL} leads to about 9% (0.0056") error in tolerance, and 33% error in C_{UL} leads to about -4% (-0.0027") error in tolerance. Although, the total cost is found to be sensitive to the errors in the estimation of C_{UL} i.e. ±8% (\$ 100) error in C_{UL} leads to ±5% (\$ 130) error in the total cost. Therefore, if manufacturer overestimates the C_{UL} by \$ 300 i.e. using 1200 \$/lb instead of the actual value of 900 \$/lb, it forces the use of lower tolerance value i.e. 0.0643" instead of 0.0674" leading to increased cost of production by \$ 65 (\$ 917- \$ 852) per spar.

Table 10 Sensitivity of total cost and optimal tolerance to uncertainty in C_{UL}

$C_{UL}(\Delta C_{UL})$	$C_{total}(\Delta C_{total})$	$C_{prod}(\Delta C_{prod})$	T	$\psi(C_{UL})$	$\psi(C_{total})$	$\psi(T)$	$\frac{\psi(C_{total})}{\psi(C_{UL})}$	$\frac{\psi(T)}{\psi(C_{UL})}$
\$(\$)	\$(\$)	\$(\$)	inch	Logarithmic derivative			Sensitivity	
800 (-400)	1939(-536)	810 (-107)	0.0699	-33%	-22%	9%	0.650	-0.261
900 (-300)	2078(-397)	852 (-65)	0.0674	-25%	-16%	5%	0.643	-0.193
1000 (-200)	2212(-263)	877 (-40)	0.0661	-17%	-11%	3%	0.638	-0.168
1100 (-100)	2345(-130)	899 (-18)	0.0651	-8%	-5%	1%	0.633	-0.149
1200	2475	917	0.0643	0	0	0	0	0
1300	2604	937	0.0635	8%	5%	-1%	0.625	-0.149
1400	2732	956	0.0628	17%	10%	-2%	0.622	-0.140
1500	2858	974	0.0622	25%	15%	-3%	0.619	-0.131
1600	2983	993	0.0616	33%	21%	-4%	0.616	-0.126

Sensitivity to uncertainty in the QN cost

The cost of quality note represents the average cost involved in reviewing and resolving the two types of quality problems for a single fastener. It captures the cost incurred due to utilization of engineering and labor resources, and was estimated to be $ 107.5 (nominal) per QN. However, there can be some errors/uncertainty involved with the estimation of C_{QN}, so it is important to evaluate the impact of such errors on the optimal tolerance and total cost. The sensitivity results are shown in Table11. We found that an optimal tolerance is not sensitive to the errors in C_{QN} i.e. about 50% ($ 53.5) error in *CQN* leads to about 13% (0.0083") error in optimal tolerance. Also, total cost is approximately half as sensitive to the errors in C_{QN} as to C_{UL}. So, if manufacturer underestimates the C_{QN} by 50% (using $ 107.5 instead of the actual value of $ 161.3), it results in a lower tolerance value (0.0643" instead of 0.0688") that leads to increase in the cost of production by $ 126 ($1043 - $ 917) per spar.

Table 11 Sensitivity of total cost and optimal tolerance to uncertainty in C_{QN}

$C_{QN}(\Delta C_{QN})$	$C_{total}(\Delta C_{total})$	$C_{prod}(\Delta C_{prod})$	T	$\psi(C_{QN})$	$\psi(C_{total})$	$\psi(T)$	$\frac{\psi(C_{total})}{\psi(C_{QN})}$	$\frac{\psi(T)}{\psi(C_{QN})}$
$($)	$($)	$($)	in.	Logarithmic derivative			Sensitivity	
53.8	2081	690	0.0574	-50%	-16%	-11%	0.318	0.215
67.2	2194	752	0.0595	-38%	-11%	-7%	0.304	0.199
80.6	2295	809	0.0613	-25%	-7%	-5%	0.292	0.187
94.1	2388	864	0.0629	-13%	-4%	-2%	0.283	0.174
107.5	2475	917	0.0643	0	0	0	0	0
120.9 (13.4)	2558(83)	968(51)	0.0656	13%	3%	2%	0.267	0.162
134.4 (26.9)	2637(162)	1013(96)	0.0670	25%	7%	4%	0.260	0.168
147.8 (40.3)	2711 (236)	1043(126)	0.0688	38%	10%	7%	0.254	0.187
161.3 (53.5)	2779 (304)	1019 (102)	0.0726	50%	12%	13%	0.245	0.258

Sensitivity to uncertainty in the cost of aluminum

The cost of aluminum C_{Al} is another source of uncertainty that may have significant impact on the selection of optimal tolerance and corresponding total cost. We used the nominal value of 5.50 $/lb for C_{Al} and checked the sensitivity to fluctuations between -55% (2.5 $/lb) and 100% (11 $/lb). The results of the sensitivity are presented in Table 12. We found that optimal tolerance and total cost are not sensitive to the fluctuations in the C_{Al}.

Table 12 Sensitivity of total cost and optimal tolerance to uncertainty in C_{Al}

$C_{Al}(\Delta C_{Al})$	$C_{total}(\Delta C_{total})$	$C_{prod}(\Delta C_{prod})$	T	$\psi(C_{Al})$	$\psi(C_{total})$	$\psi(T)$	$\frac{\psi(C_{total})}{\psi(C_{Al})}$	$\frac{\psi(C_{total})}{\psi(C_{Al})}$
$($)	$($)	$($)	in.	Logarithmic derivative			Sensitivity	
2.5	2345	767	0.0651	-55%	-5%	1%	0.097	-0.023
4	2410	842	0.0647	-27%	-3%	1%	0.097	-0.023
5.5	2475	917	0.0643	0	0	0	0	0
7	2540 (65)	992 (70)	0.0639	27%	3%	-1%	0.096	-0.023
8.5	2605 (130)	1066 (149)	0.0635	55%	5%	-1%	0.096	-0.023
10	2669 (194)	1137 (220)	0.0632	82%	8%	-2%	0.096	-0.021
11	2712 (237)	1185 (268)	0.0630	100%	10%	-2%	0.095	-0.020

Sensitivity to uncertainty in edge distance deviation data

The data for edge distance deviation (Δe) were collected from 8 wing assemblies (8164 samples) that only represent about 2.3 % of the expected number of aircrafts (350) to be produced. There are various sources of uncertainties that can change the scale (s) and location (μ) of the estimated EDD distribution, which can lead to errors in the estimation of the P_{QN} and P_{CV}. It is important to quantify the impact of such uncertainties on the optimal tolerance and total cost. The three possible sources of uncertainties are,

1. Degradation in the accuracy of the assembly tools (e.g. jigs) over the period of time will increase the manufacturing variability.
2. Measurement errors in ascertaining the edge distance of the fastener holes.
3. Limited amount of data.

In order to investigate the sensitivity of the optimal tolerance to the uncertainty in edge distance distribution data, we chose to vary the scale parameter (s) of the estimated logistic distribution from its nominal value by ±50%. The sensitivity results are presented in the Table 13. We found that both optimal tolerance and total cost are sensitive to the errors in s i.e. about 50% error in s leads to about 39% ($ 953) error in C_{total} and 41% ($ 289) error in C_{prod}.

Table 13 Sensitivity of total cost and optimal tolerance to uncertainty in *s*

s	$C_{total}(\Delta C_{total})$	$C_{prod}(\Delta C_{prod})$	T	$\psi(s)$	$\psi(C_{total})$	$\psi(T)$	$\frac{\psi(C_{total})}{\psi(s)}$	$\frac{\psi(T)}{\psi(s)}$
in.	$($)	$($)	in.	Logarithmic derivative			Sensitivity	
0.0069	1414	421	0.0410	-50%	-43%	-40%	0.86	0.80
0.0086	1692	492	0.0495	-38%	-32%	-30%	0.84	0.79
0.0103	1960	569	0.0574	-25%	-21%	-19%	0.83	0.75
0.0121	2222	642	0.0652	-13%	-10%	-8%	0.81	0.66
0.0138	2474	700	0.0732	0	0	0	0	0
0.0155	2716 (242)	770 (70)	0.0803	13%	10%	10%	0.78	0.80
0.0172	2956 (482)	846 (146)	0.0871	25%	20%	21%	0.78	0.83
0.0190	3194 (720)	916 (216)	0.0940	38%	29%	31%	0.78	0.82
0.0207	3427 (953)	989 (289)	0.1006	50%	39%	41%	0.77	0.83

Sensitivity to uncertainty in hole diameter deviation data

For the same reasons discussed above, it is desirable to check the impact of uncertainty in hole diameter distribution on the optimal tolerance and total cost. The nominal value of the probability of oversizing a fastener i.e. $P(\Delta d>0)$ or P_{HO} is 0.001724, and for lower bound it is assumed that it reduces to zero (100% decrease) and for upper bound it is assumed that it increases by a factor of 100%. For simplicity, it is assumed that any change in the $P_{HO}$is equally distributed among all the possible over size values (i.e. from 1/64 to 13/64). The sensitivity results shown in Table 14 indicate that optimal tolerance and total cost are not sensitive to the uncertainties in hole diameter deviation data.

Table 14 Sensitivity of total cost and optimal tolerance to uncertainty in P_{HO}

P_{HO}	$C_{total}(\Delta C_{total})$	$C_{prod}(\Delta C_{prod})$	T	$\psi(P_{HO})$	$\psi(C_{total})$	$\psi(T)$	$\frac{\psi(C_{total})}{\psi(P_{HO})}$	$\frac{\psi(C_{total})}{\psi(P_{HO})}$
	$($)	$($)	in.	Logarithmic derivative			Sensitivity	
0	2392	628	0.0728	-100%	-3%	-0.6%	0.03	0.01
0.0009	2433	664	0.0730	-50%	-2%	-0.3%	0.03	0.01
0.0013	2453	682	0.0731	-25%	-1%	-0.1%	0.03	0.01
0.0017	2474	700	0.0732	0	0	0	0	0
0.0022	2494 (20)	717 (17)	0.0734	25%	1%	0.2%	0.03	0.01
0.0026	2514 (40)	735 (35)	0.0735	50%	2%	0.3%	0.03	0.01
0.0034	2554 (80)	768 (68)	0.0738	100%	3%	0.8%	0.03	0.01

Concluding Remarks

We have demonstrated the use of integrated "Design for Customer" approach that combined the quality cost, manufacturing cost and performance cost to optimize the manufacturing tolerance for a wing spar lap joint, under manufacturing uncertainty/errors associated with the location and size of the fastener holes. The lap joint was designed under damage tolerance/fatigue design philosophy. An alternative formulation for the total cost that ignored the performance cost was also studied. As expected, including performance cost gave a spar design that was lighter but expensive. We then showed that as the aircraft size grows bigger it becomes more important for a manufacturer to incorporate the performance cost. A sensitivity analysis was performed that identified the input variables that have significant impact on the optimal tolerance and corresponding total cost. We found that uncertainty in the cost of useful load and cost of quality notification can lead to noteworthy errors in total cost. The uncertainty in edge distance deviation data lead to significant errors in both optimal tolerance and total cost.

Future Work

The sensitivity analysis identified the input variables that can lead to significant errors in the optimal tolerance and total cost. We plan to incorporate the uncertainties associated with these variables in the tolerance optimization procedure.

Acknowledgement

We are thankful to the NSF grant CMMI-1131103, Resource Allocation for Airliner Safety and Cessna Aircraft Company (Wichita, KS) for supporting and helping us with the data required for this study. The invaluable guidance and feedback from Chris Hurst (Engineer Specialist- Sr., F&DT), Dan Kalal (Engineering Manager, F&DT), and Bobbie Kroetch (Engineer- Sr., F&DT) at Cessna need special thanks.

Appendices

Appendix A

Interpolation accuracy

The accuracy of the 2D interpolation function to predict the initial inspection interval during Monte Carlo Simulationisestimated by building a set of test points shown in Figure. The interpolation function is first approximated by using 126 interpolation nodes (spaced at Δe =0.025") at which actual initial inspection interval values are known and then initial inspection interval were predicted at the test points (spaced at Δe =0.005"). The actual crack growth analyses are also performed at these test points by using AFGROW. The root mean square error (RMSE) is calculated by using the following formula,

$$RMSE = \sqrt{\frac{\sum_{i=1}^{n}\left(I_{ini-AFGROW} - I_{ini-Interp}\right)_i^2}{n}} \quad . \tag{21}$$

The RMSE for all the 21 interpolation functions corresponding to a particular tolerance value ranged between 16-19 flight hours (FH). A closer look on the test points between point A and B shown in the left corner of Figure 18 (a) is in shown in Figure 18 (b). The RMSE for the points (spaced at 0.001") shown in Figure (b) is calculated to be 14 FH with the max error of 32 FH and range of 1033 FH. A reasonable estimate of the interpolation accuracy can be calculated by dividing the RMSE by the range i.e. 14/1033 = 1.36 %, which is quite good. Also, Figure 18 (b) shows that AFGROW generated results are bit noisy and linear interpolation predictions might actually be more accurate than the AFGROW results at the test points.

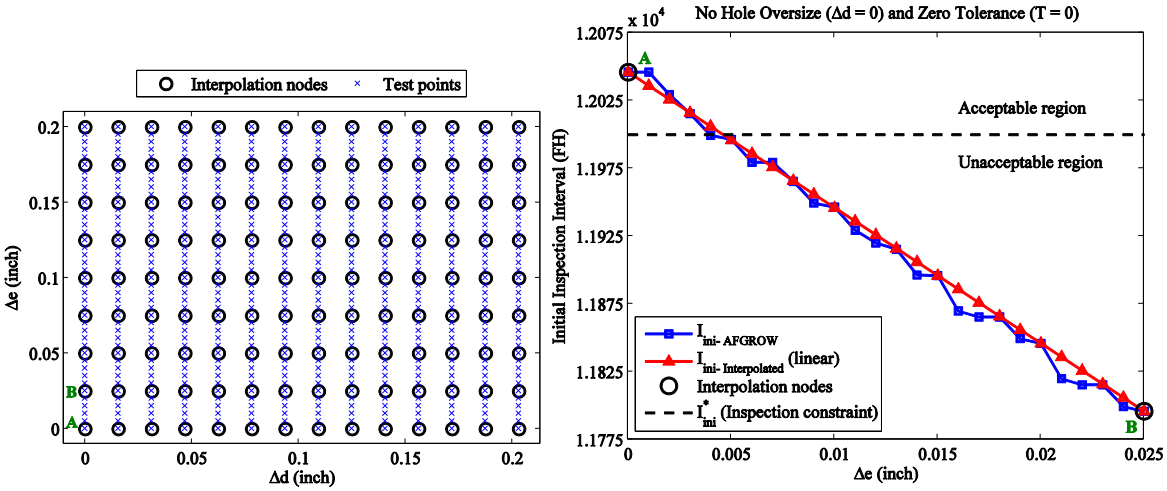

Fig. 18 (a) Sample deviation space, (b) Interpolation between point A and B shown in (a)

Appendix B

Crack Growth Analysis

The structure shown in Figure 19 is a further simplification of the joint shown in Figure 3 (b), with only lower spar cap and strap needed to execute a crack growth analysis. The lap joint transfers load *P* lbs. i.e. applied reference gross stress $\sigma_{ref\text{-}gross} = P/wt$ Ksi, with each fastener picking up R_i lbs. and bypassing $P\text{-}\sum R_i$ lbs. of load. The proportion of the total load picked by each fastener depends upon the fastener flexibility, which is calculated by modifying the analytical relationships given in[10] for the single shear lap joint shown in Figure 19. These relationships yield reasonably accurate results for the fastener loads i.e. within 10% of the FEA results. The resulting fastener load distribution is shown in Figure 19 with ($R_2=R_4$&$R_1=R_5$); it is clear that end fasteners (R_1&R_5) are the most fatigue critical as they pick up the maximum load. Therefore, crack growth analyses are only executed for the 1st fastener and it is assumed that all the fastener holes on the wing spar have similar crack growth characteristics.

The loads calculated by analytical relationships are then used to find the bearing and bypass stress ratios that serve as inputs to the AFGROW analysis. These ratio are calculated for the end fasteners by the following equations,

$$\eta_{TR1} = \frac{\sigma_{by1}}{\sigma_{ref-gross}} = \frac{P - R_1}{P}, \quad \eta_{BrgR1} = \frac{\sigma_{brg1}}{\sigma_{ref-gross}} = \frac{R_1}{P}\left(\frac{w}{d}\right). \tag{22}$$

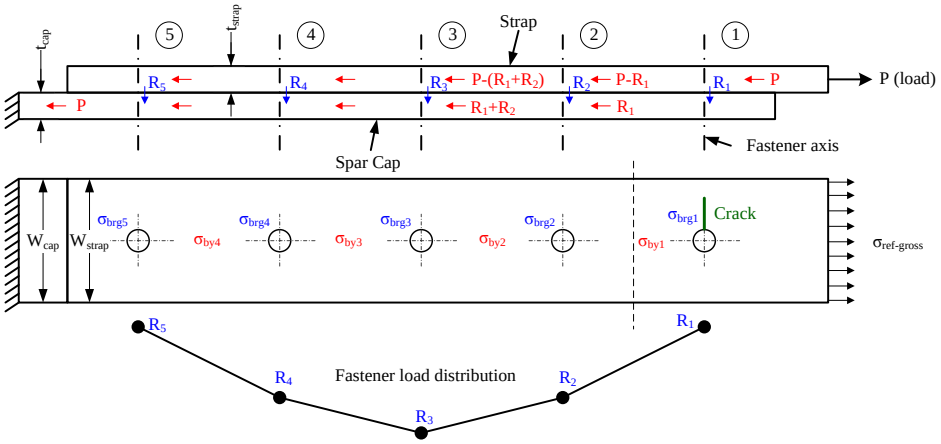

Fig. 19 Fastener load distribution and stresses.

We have used the single corner crack model to execute the crack growth analysis as shown in Figure 20. The initial crack length of $A = C = 0.05$" is used. The crack is grown under a variable amplitude stress spectrum that is taken from a wing spar location of a business jet. It grows steadily till final crack length a_f and unzips after that leading to the fast fracture. The stress spectrum used in the analysis is 100 flight hours long, and initial inspection interval is estimated by dividing the total number of flight hours it takes to reach a_f by a factor of 2.

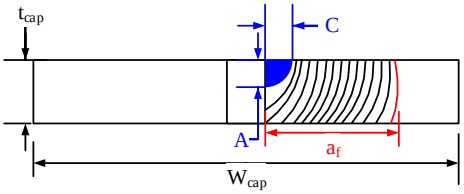

Fig. 20 Corner crack model used in the AFGROW

References

[1] Chen, T.C., Fisher W., "A GA-based search method for the tolerance allocation problem", Artificial Intelligence in Engineering, Vol. 14, Issue 2, 2000, pp. 133-141.

[2] Zhang C., Wang H.P., "Integrated tolerance optimization with simulated annealing",The International Journal of Advanced Manufacturing Technology, Vol. 8, No. 3, 1993,pp. 167-174.

[3] Ye, B., Salustri, F.A., "Simultaneous tolerance synthesis for manufacturing and quality",Research in Engineering Design, Vol. 14, No. 2, 2003, pp. 98-106.

[4] Muthu, P., Dhanalakshmi, V., Sankaranarayanaswamy, K., "Optimal tolerances design of assembly for minimum quality loss and manufacturing cost using metaheuristic algorithms", International Journal of Advanced Manufacturing Technology, Vol. 44, No. 11-12, 2009, pp. 1154-1164.

[5]Curran, R., Kundu, A., Raghunathan, S., Eakin, D., McFadden, R., "Influence of Manufacturing tolerance on aircraft direct operating cost (DOC)", Journal of Materials Processing Technology", Vol. 138, Issue. 1-3, 2003, pp. 208-213.

[6] Curran, R., Kundu, A., "Design for Customer", Article retrieved from http://www.icas.org/ICAS_ARCHIVE/ICAS2004/PAPERS/122.PDF, on March 19, 2013.

[7] Website, http://www.aircraftcompare.com/

[8] Hong Y. S., T. C. Chang, "A Comprehensive Review of Tolerancing Research", International Journal of Production Research, Vol. 40, No. 11, 2002, pp. 2425-2459.

[9] Cleveland F. A., "Size Effects in Conventional Aircraft Design", Journal of Aircraft, 33rd Wright Brothers Lecture, Vol. 7, No. 6, Nov –Dec 1970.

[10] Tate B., Rosenfeld S. J., "Preliminary Investigation of the Loads Carried by Individual Bolts in Bolted Joints", Technical Note, National Advisory Committee for Aeronautics (NACA TN. 1051), May 1946.